Supplementary Information

A crystalline molecular gyrotop with germanium junctions between a phenylene rotor and alkyl spokes

Yusuke Inagaki,[a] Kentaro Yamaguchi,[b] and Wataru Setaka,*[,a]

[a] *Division of Applied Chemistry, Faculty of Urban Environmental Sciences, Tokyo Metropolitan University, 1-1 Minami-Osawa, Hachioji, Tokyo 192-0397, Japan*

[b] *Faculty of Pharmaceutical Sciences at Kagawa Campus, Tokushima Bunri University, 1314-1 Shido, Sanuki, Kagawa 769-2193, Japan*

1. Copies of NMR Spectra for All New Compounds

a. Spectra of Ethoxytris(7-octenyl)germane (3)

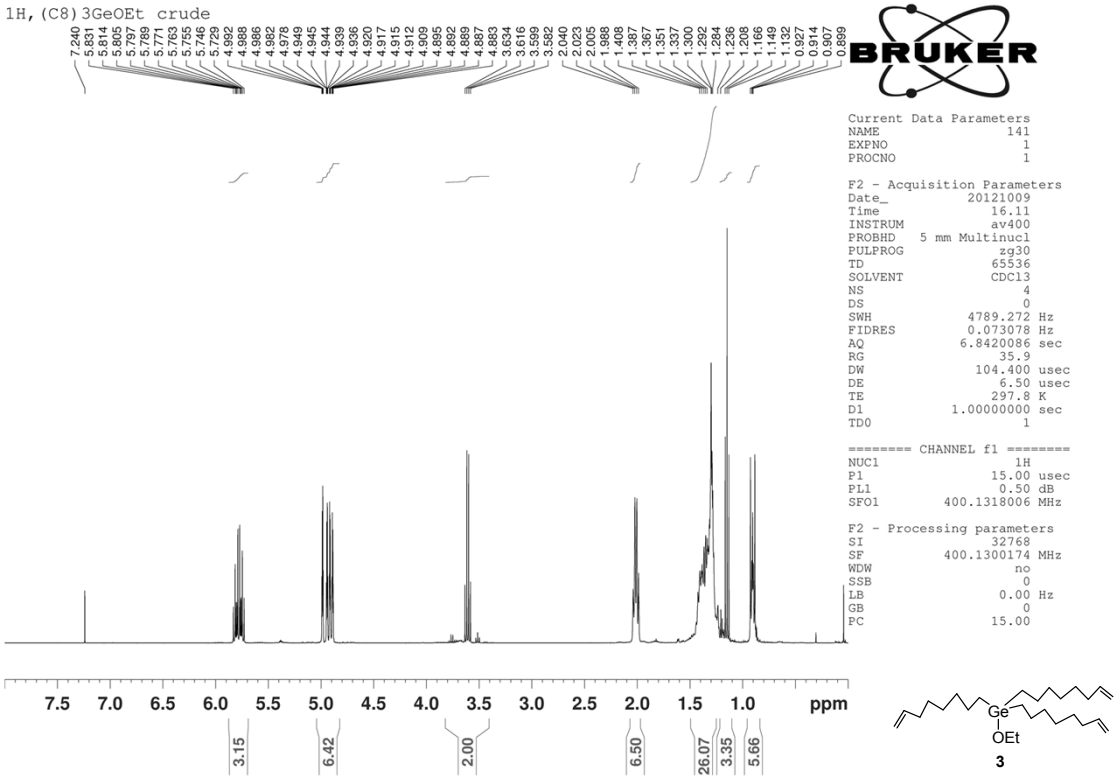

Fig S1. ^{1}H NMR spectrum of Ethoxytris(7-octenyl)germane (**3**) in $CDCl_3$.

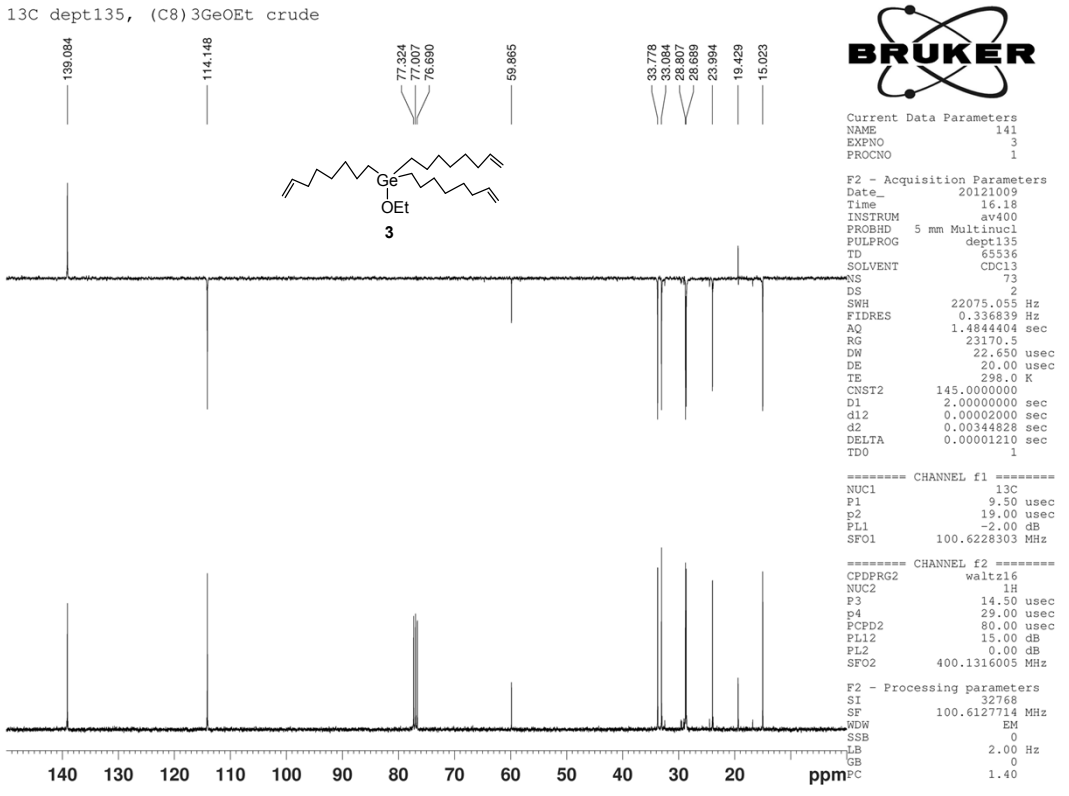

Fig S2. ^{13}C NMR spectrum of Ethoxytris(7-octenyl)germane (**3**) in $CDCl_3$.

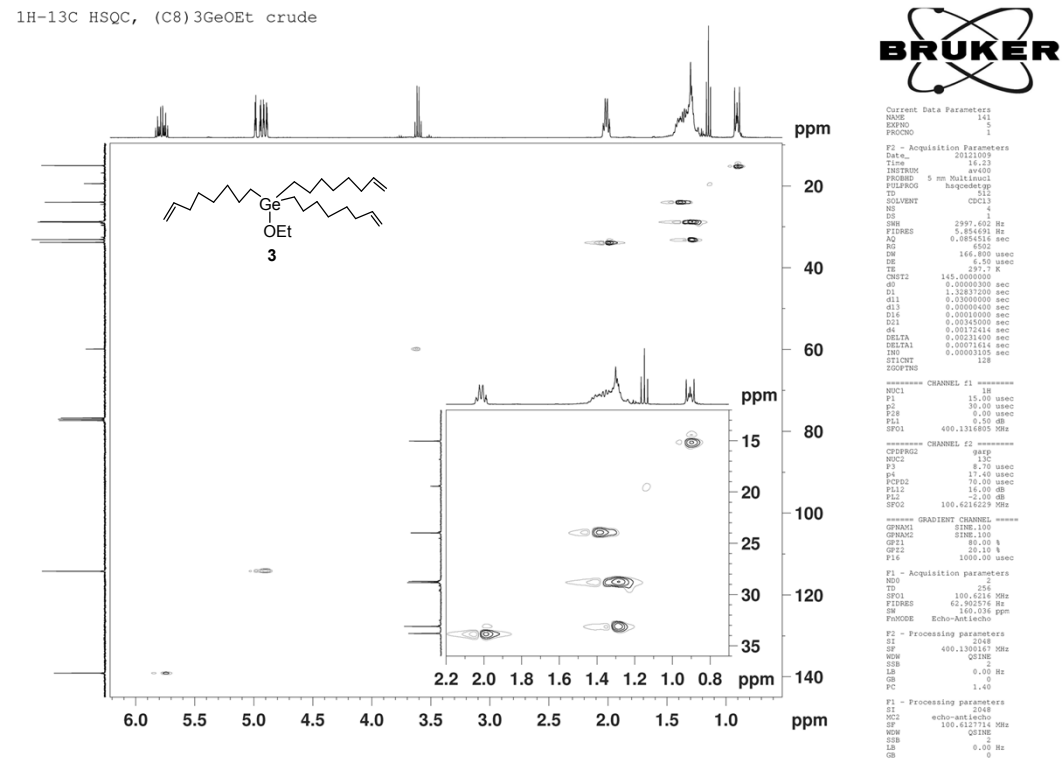

Fig S3. ^{1}H-^{13}C hsqc NMR spectrum of Ethoxytris(7-octenyl)germane (**3**) in $CDCl_3$.

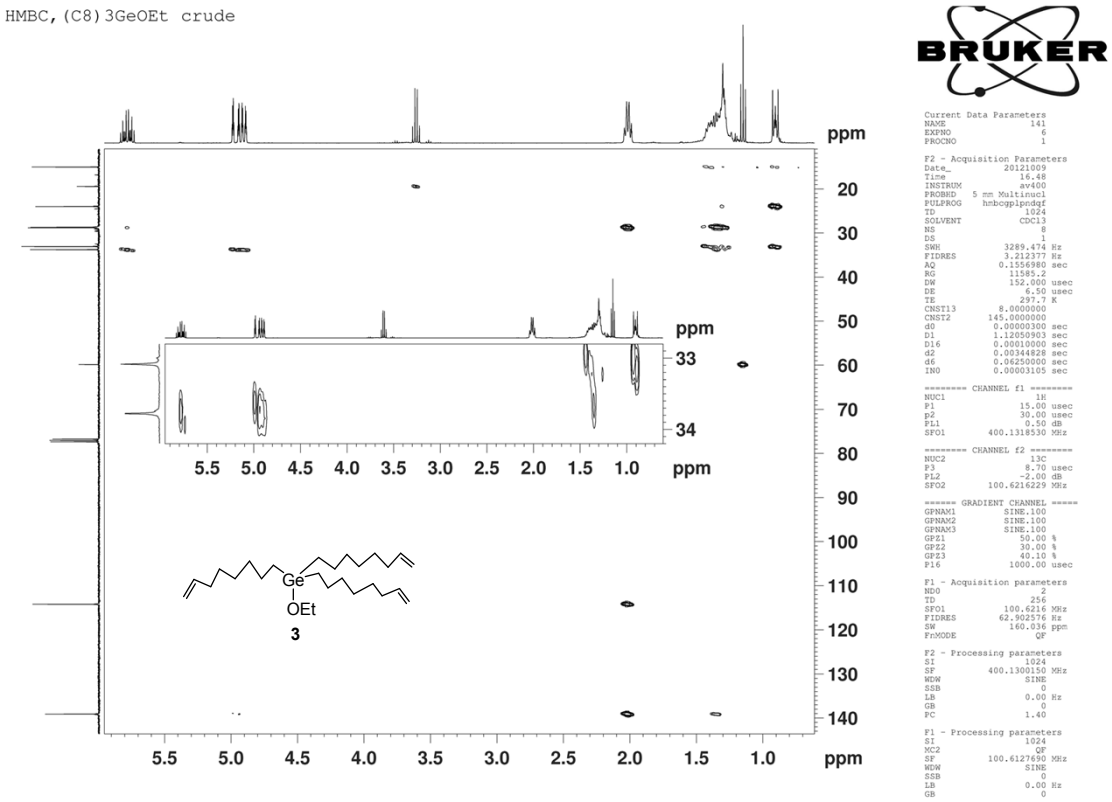

Fig S4. ^{1}H-^{13}C hmbc NMR spectrum of Ethoxytris(7-octenyl)germane (**3**) in $CDCl_3$.

b. Spectra of Chlorotris(7-octenyl)germane (4)

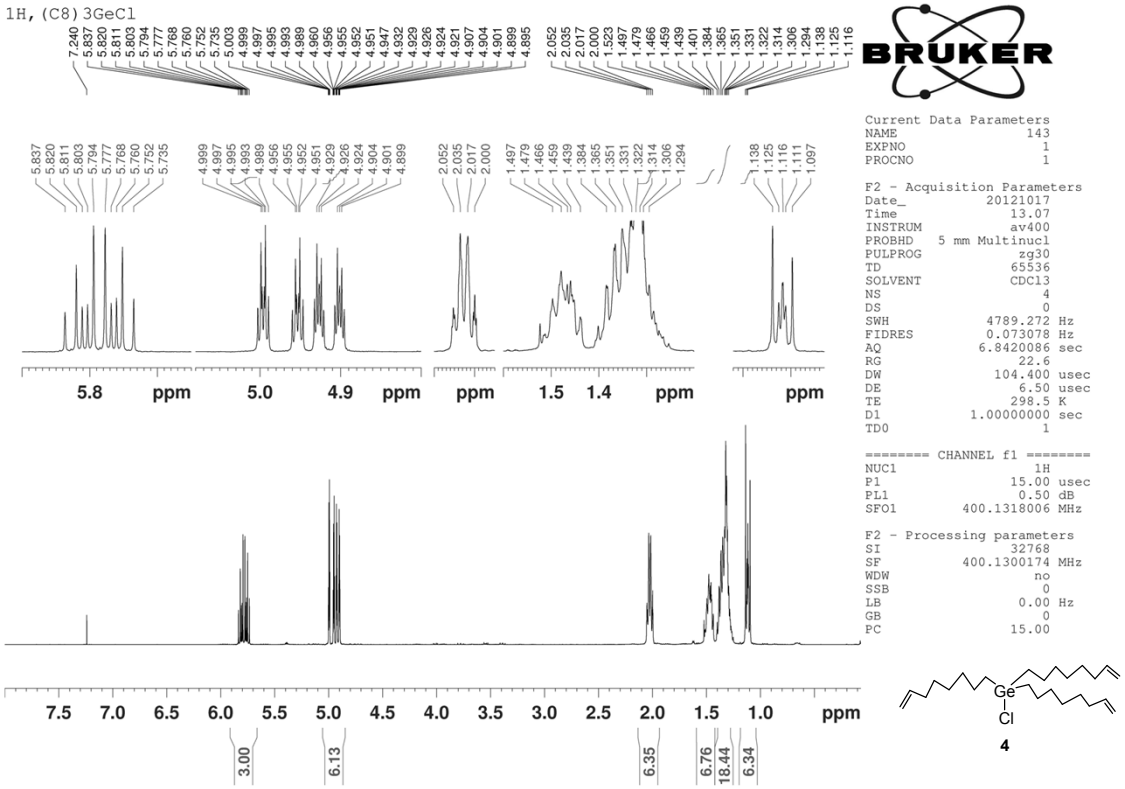

Fig S5. ^{1}H NMR spectrum of Chlorotris(7-octenyl)germane (**4**) in $CDCl_3$.

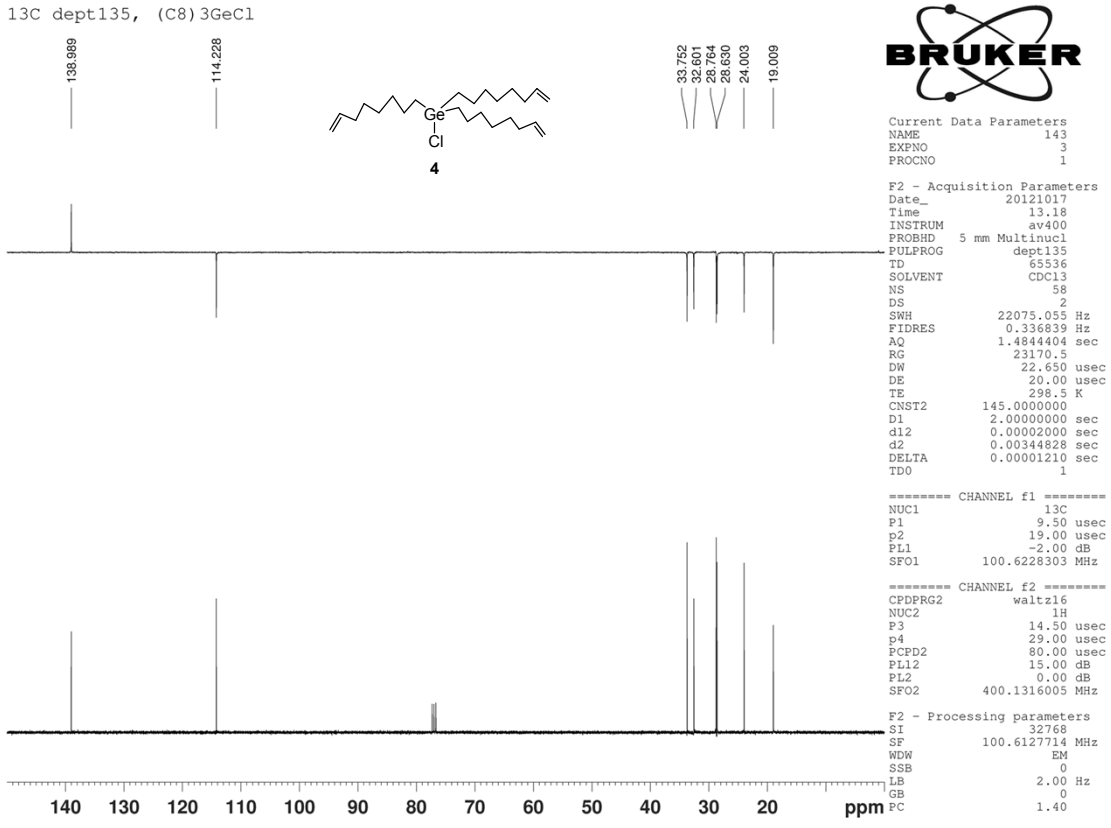

Fig S6. ^{13}C NMR spectrum of Chlorotris(7-octenyl)germane (**4**) in $CDCl_3$.

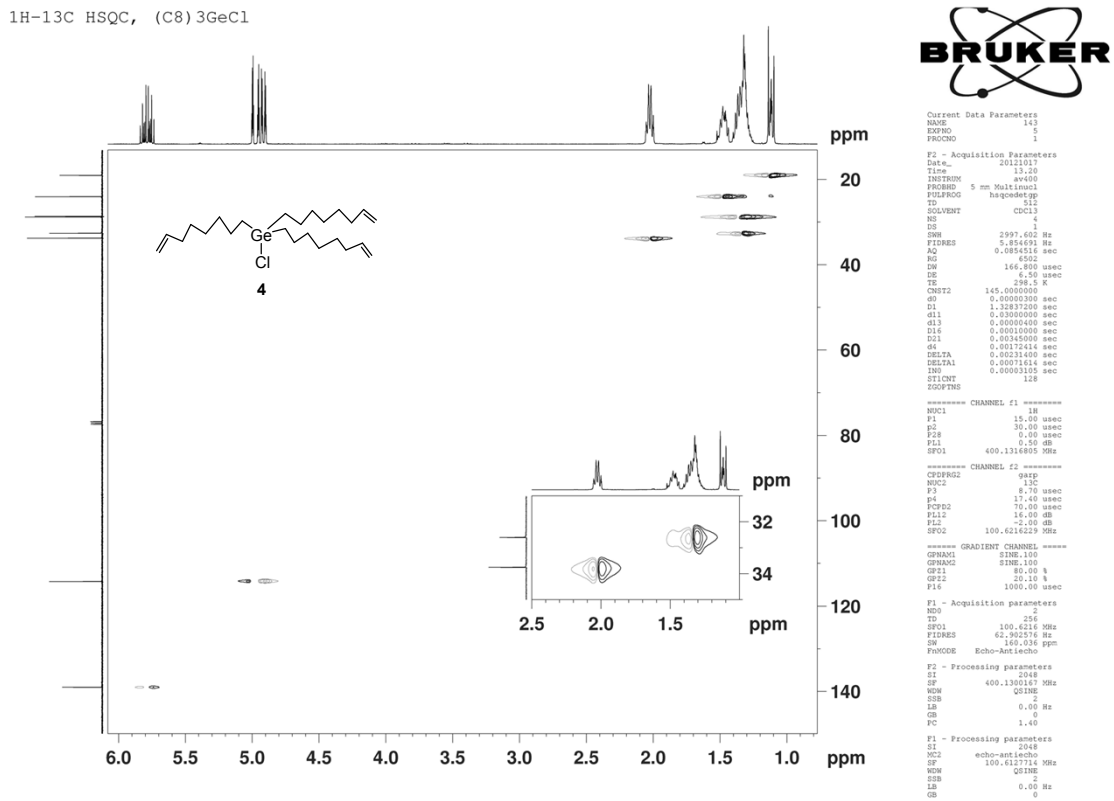

Fig S7. ^{1}H-^{13}C hsqc NMR spectrum of Chlorotris(7-octenyl)germane (**4**) in $CDCl_3$.

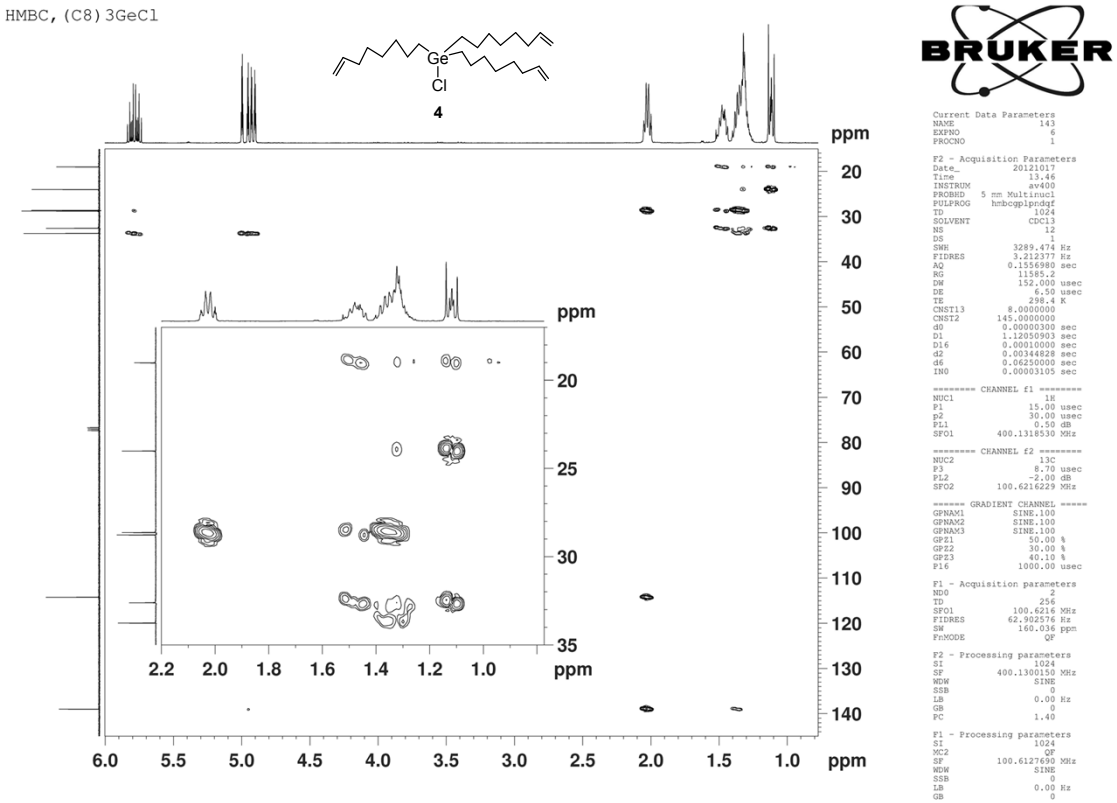

Fig S8. ^{1}H-^{13}C hmbc NMR spectrum of Chlorotris(7-octenyl)germane (**4**) in $CDCl_3$.

c. Spectra of 1,4-bis(tri-7-octenylgermyl)benzene (5)

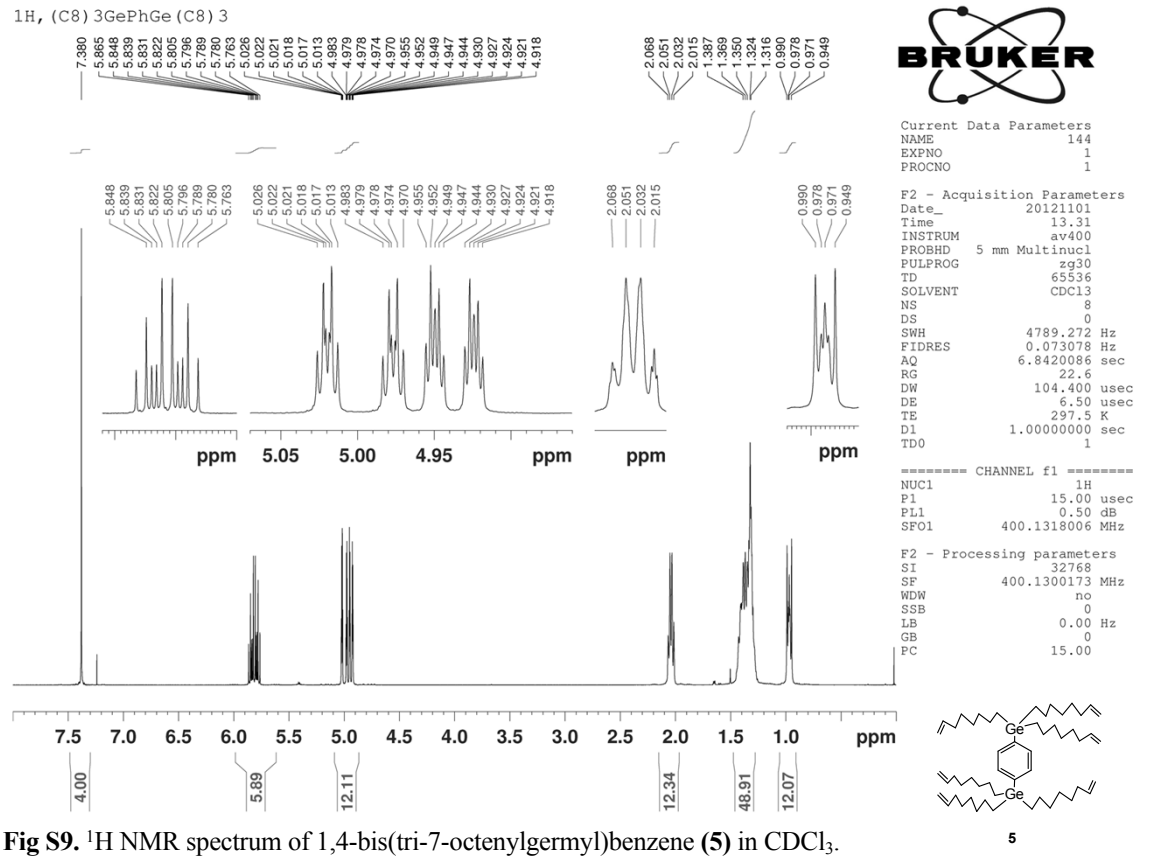

Fig S9. ^{1}H NMR spectrum of 1,4-bis(tri-7-octenylgermyl)benzene **(5)** in $CDCl_3$.

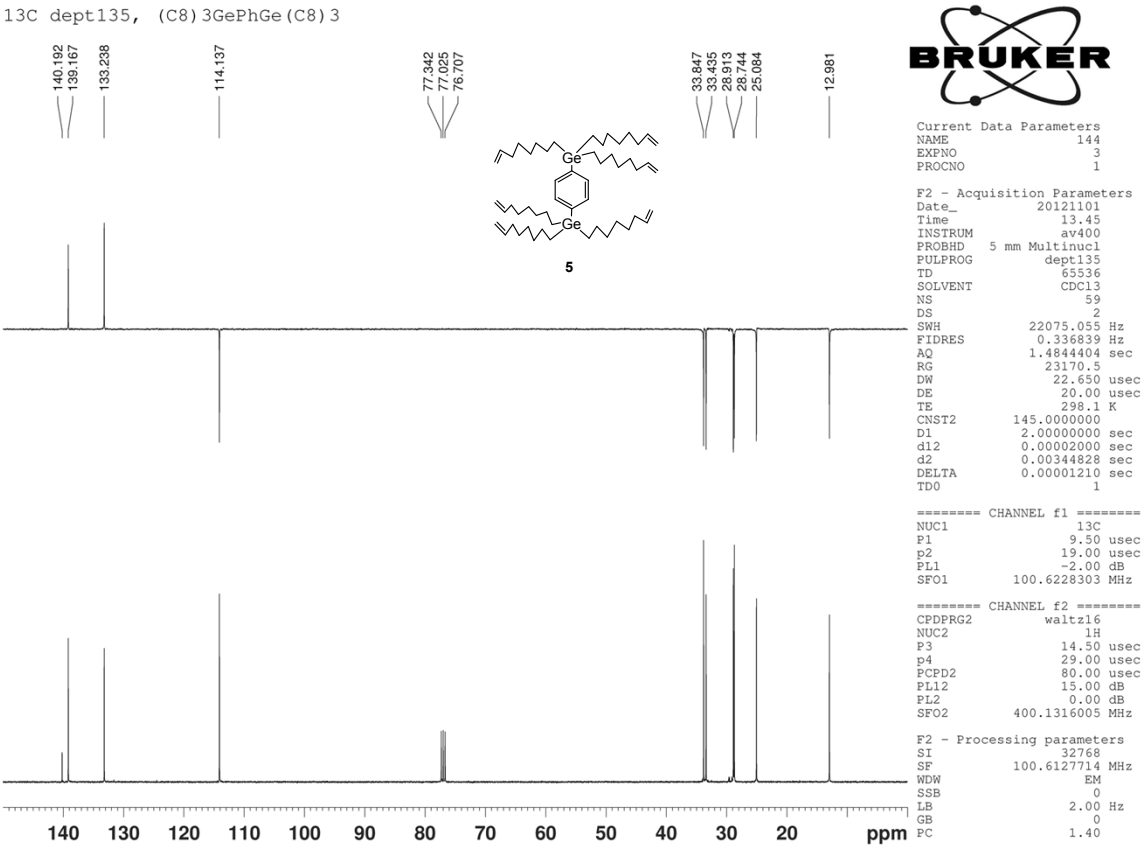

Fig S10. ^{13}C NMR spectrum of 1,4-bis(tri-7-octenylgermyl)benzene **(5)** in $CDCl_3$.

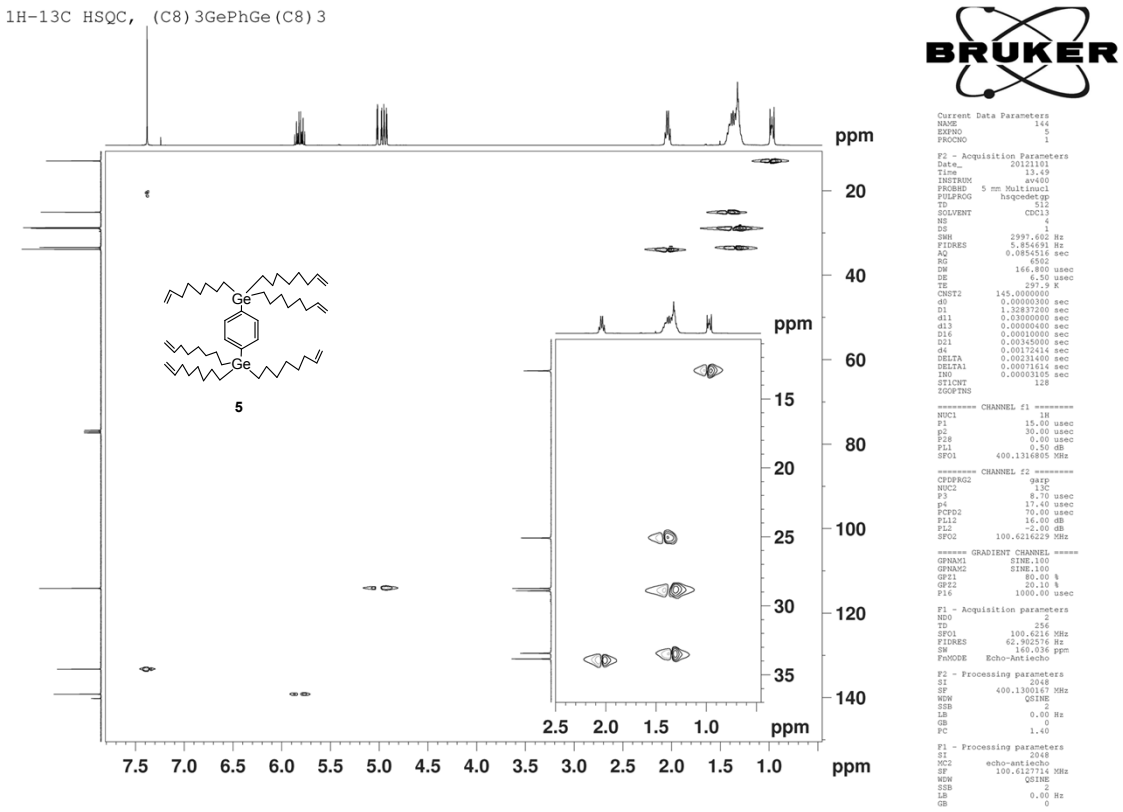

Fig S11. ^{1}H-^{13}C hmbc NMR spectrum of 1,4-bis(tri-7-octenylgermyl)benzene **(5)** in $CDCl_3$.

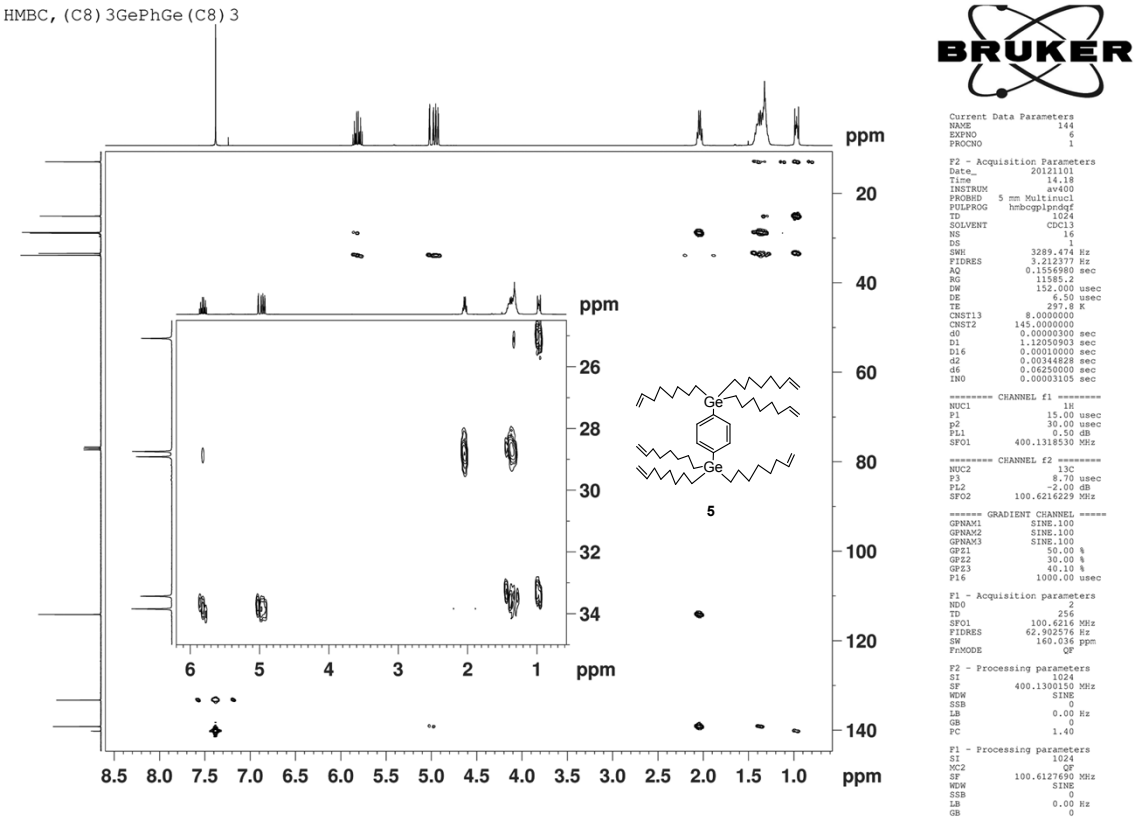

Fig S12. ^{1}H-^{13}C hsqc NMR spectrum of 1,4-bis(tri-7-octenylgermyl)benzene **(5)** in $CDCl_3$.

d. Spectra of Molecular Gyrotop (2)

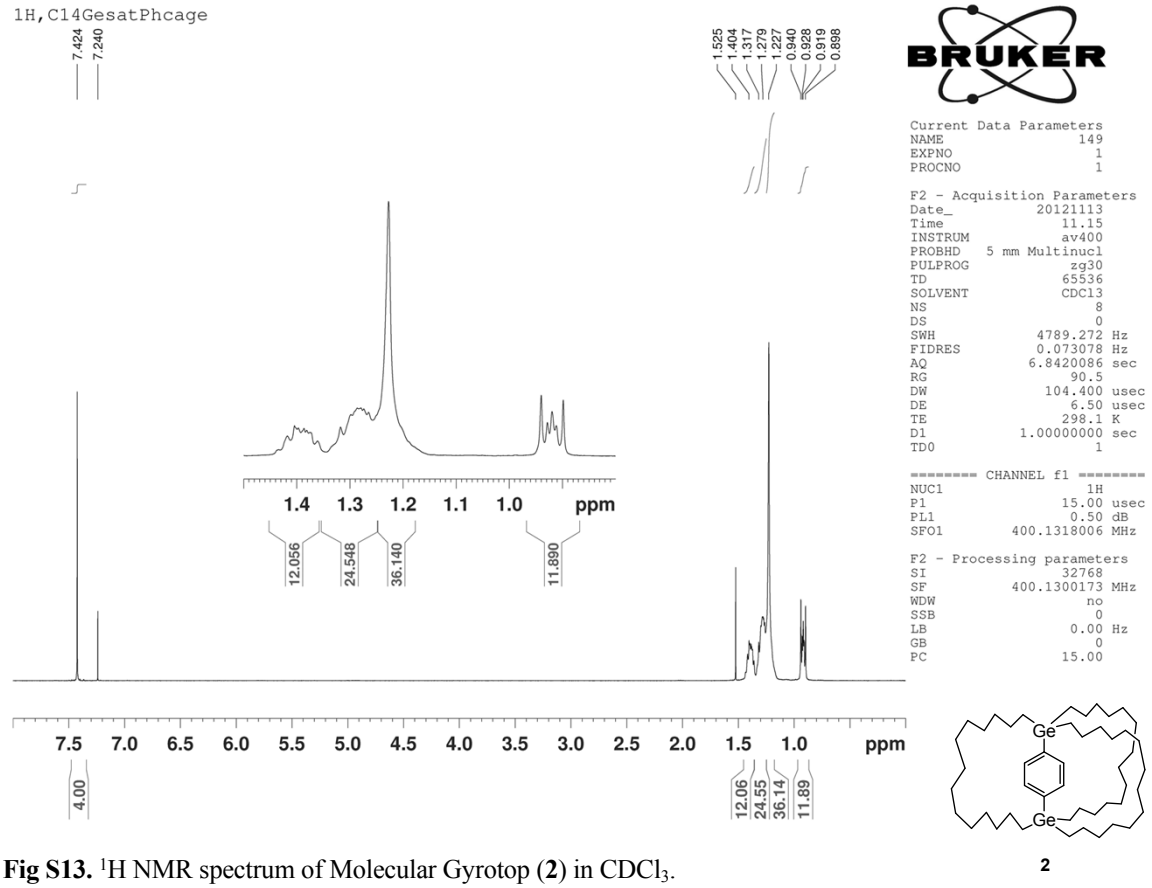


```
Current Data Parameters
NAME                  149
EXPNO                   1
PROCNO                  1

F2 - Acquisition Parameters
Date_            20121113
Time                11.15
INSTRUM             av400
PROBHD   5 mm Multinucl
PULPROG              zg30
TD                  65536
SOLVENT             CDCl3
NS                      8
DS                      0
SWH              4789.272 Hz
FIDRES           0.073078 Hz
AQ               6.8420086 sec
RG                   90.5
DW                104.400 usec
DE                  6.50 usec
TE                 298.1 K
D1             1.00000000 sec
TD0                     1

======== CHANNEL f1 ========
NUC1                   1H
P1                 15.00 usec
PL1                 0.50 dB
SFO1          400.1318006 MHz

F2 - Processing parameters
SI                  32768
SF            400.1300173 MHz
WDW                    no
SSB                     0
LB                   0.00 Hz
GB                      0
PC                  15.00
```

Fig S13. ^{1}H NMR spectrum of Molecular Gyrotop (**2**) in $CDCl_3$.

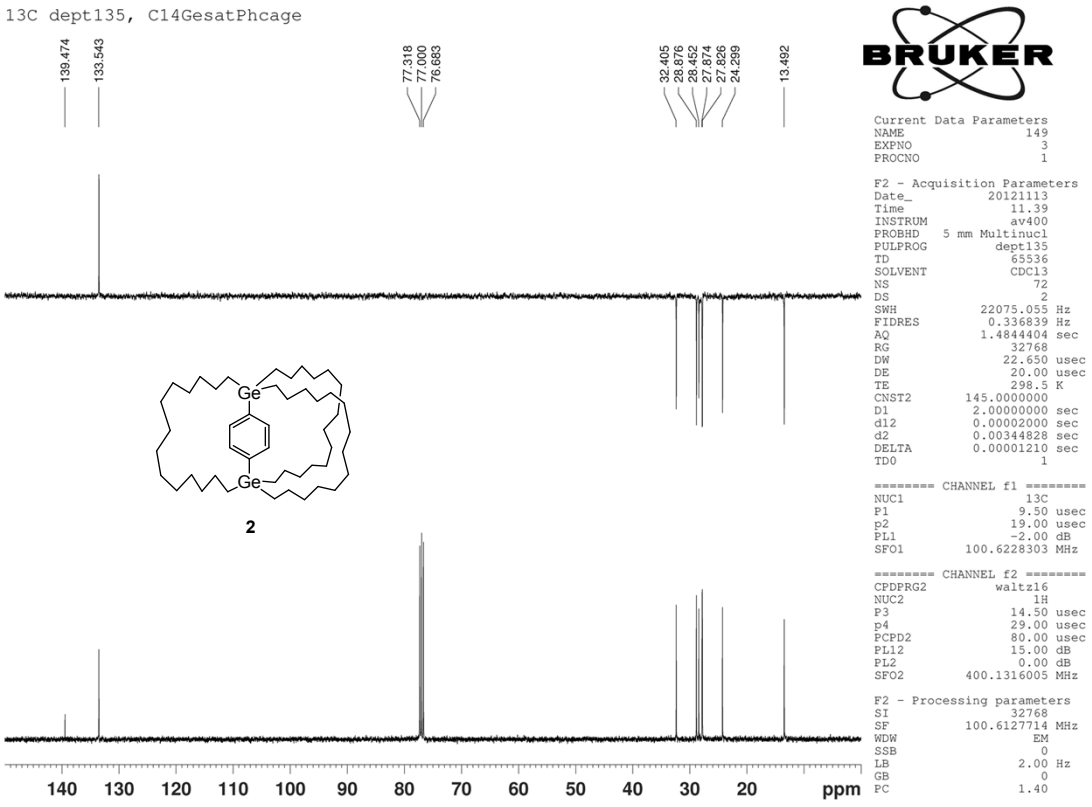


```
Current Data Parameters
NAME                  149
EXPNO                   3
PROCNO                  1

F2 - Acquisition Parameters
Date_            20121113
Time                11.39
INSTRUM             av400
PROBHD   5 mm Multinucl
PULPROG           dept135
TD                  65536
SOLVENT             CDCl3
NS                     72
DS                      2
SWH             22075.055 Hz
FIDRES           0.336839 Hz
AQ               1.4844404 sec
RG                  32768
DW                22.650 usec
DE                20.00 usec
TE                 298.5 K
CNST2         145.0000000
D1             2.00000000 sec
d12            0.00002000 sec
d2             0.00344828 sec
DELTA          0.00001210 sec
TD0                     1

======== CHANNEL f1 ========
NUC1                   13C
P1                  9.50 usec
p2                 19.00 usec
PL1                -2.00 dB
SFO1          100.6228303 MHz

======== CHANNEL f2 ========
CPDPRG2           waltz16
NUC2                   1H
P3                 14.50 usec
p4                 29.00 usec
PCPD2              80.00 usec
PL12               15.00 dB
PL2                 0.00 dB
SFO2          400.1316005 MHz

F2 - Processing parameters
SI                  32768
SF            100.6127714 MHz
WDW                    EM
SSB                     0
LB                   2.00 Hz
GB                      0
PC                  1.40
```

Fig S14. ^{13}C NMR spectrum of Molecular Gyrotop (**2**) in $CDCl_3$.

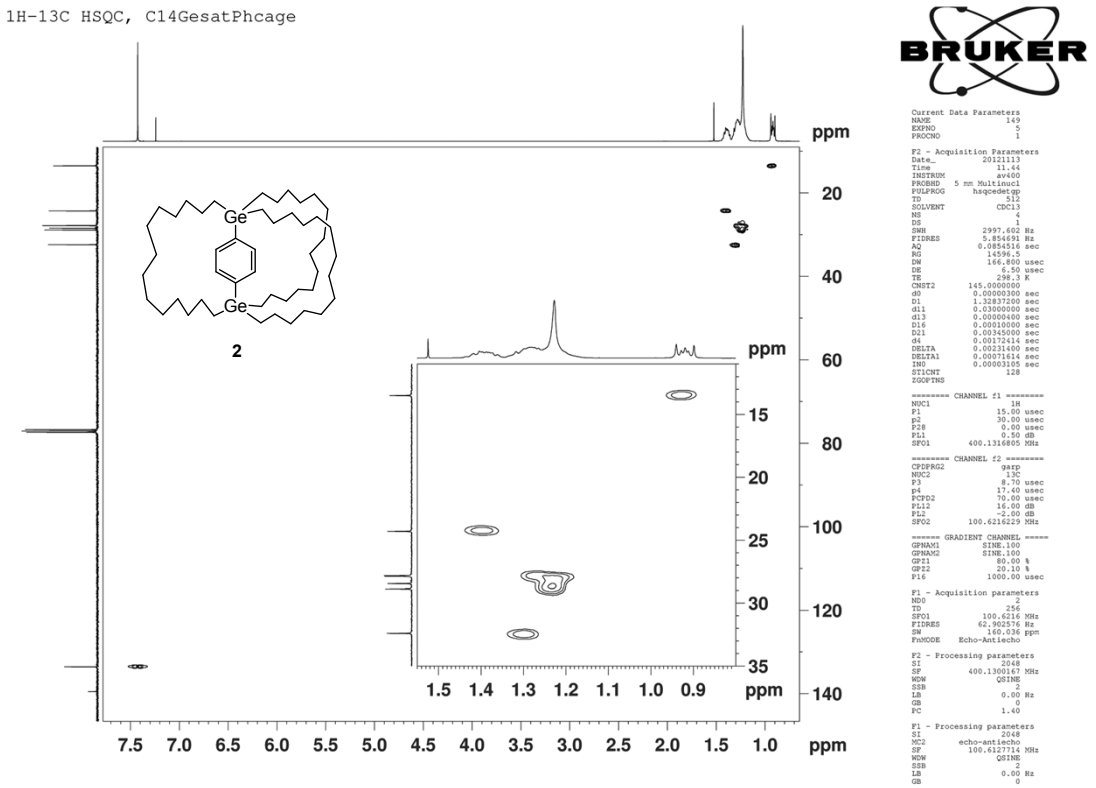

Fig S15. ^{1}H-^{13}C hsqc NMR spectrum of Molecular Gyrotop (**2**) in $CDCl_3$.

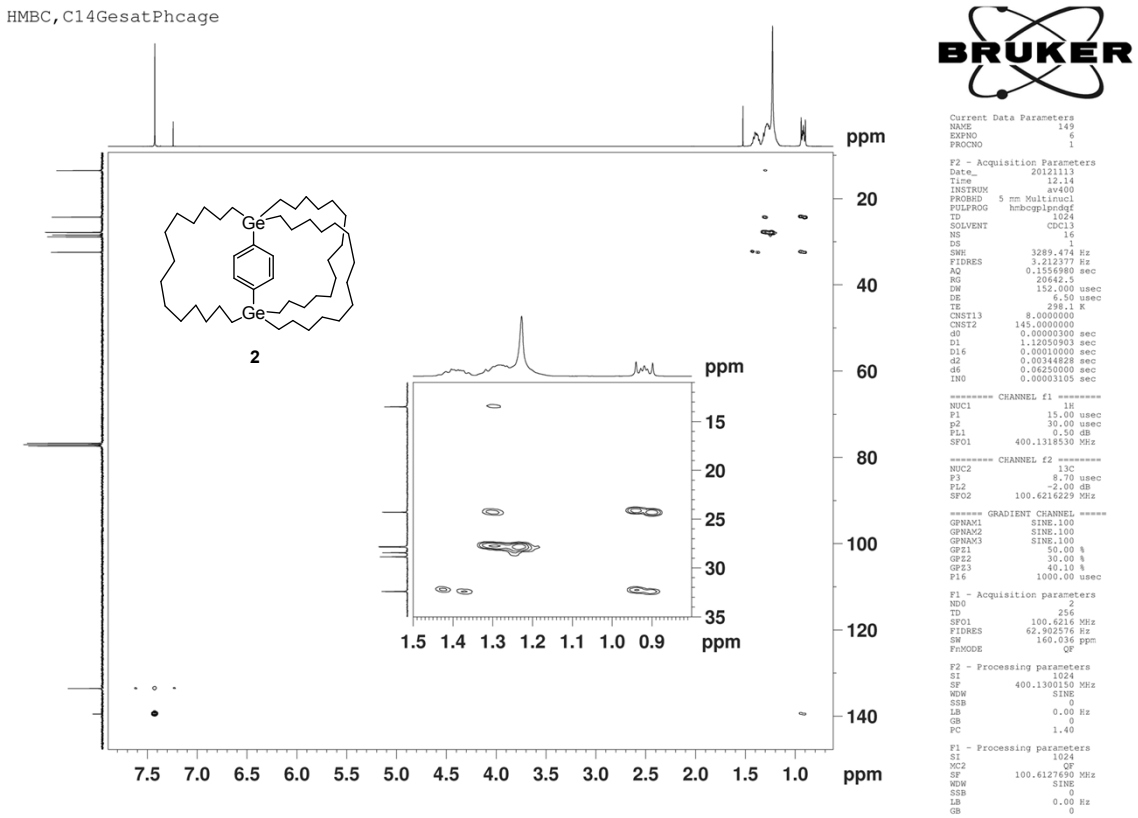

Fig S16. ^{1}H-^{13}C hmbc NMR spectrum of Molecular Gyrotop (**2**) in $CDCl_3$.

e. Spectra of Molecular Gyrotop Isomer (2i)

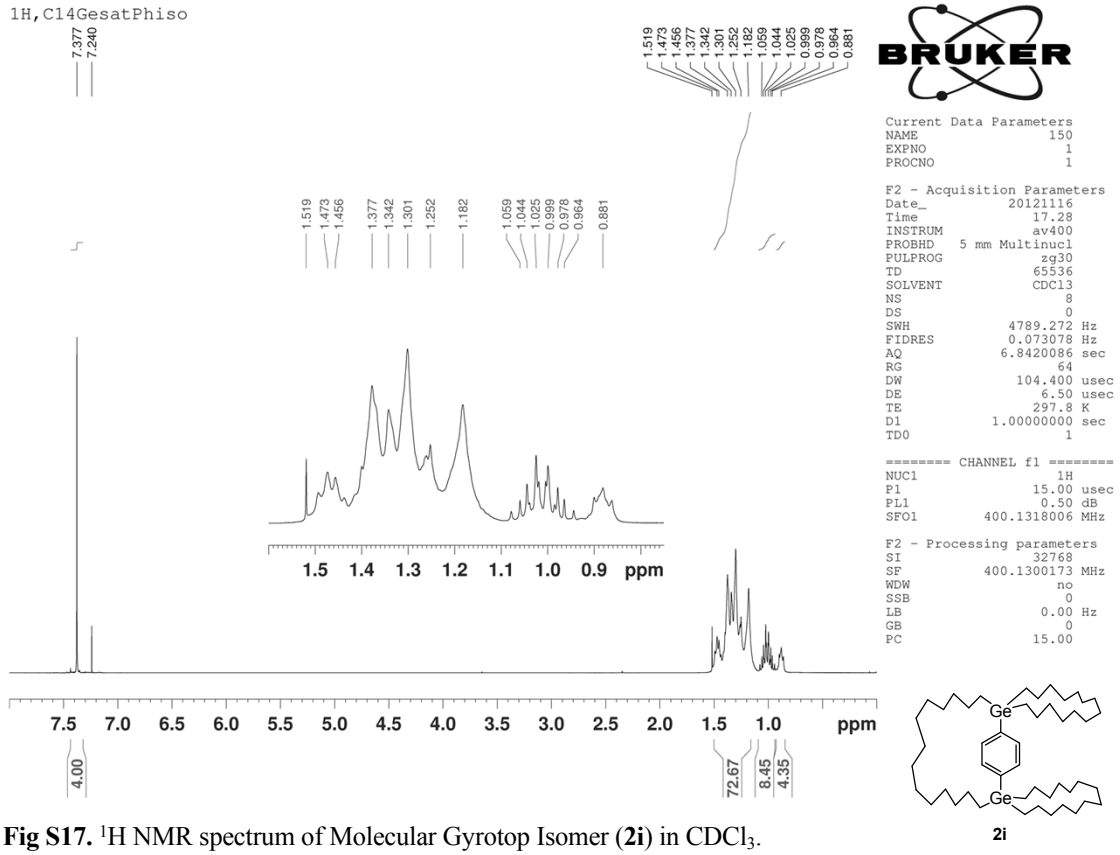

Fig S17. ^{1}H NMR spectrum of Molecular Gyrotop Isomer (**2i**) in $CDCl_3$.

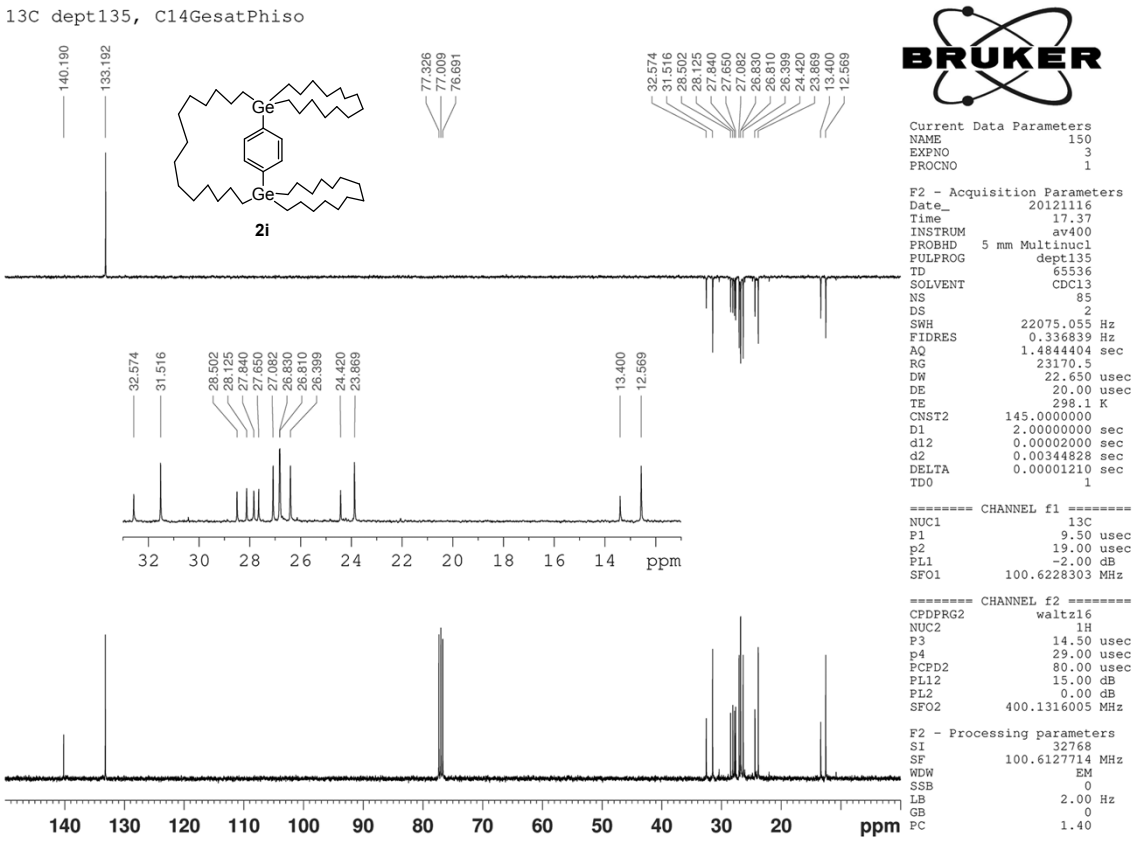

Fig S18. ^{13}C NMR spectrum of Molecular Gyrotop Isomer (**2i**) in $CDCl_3$.

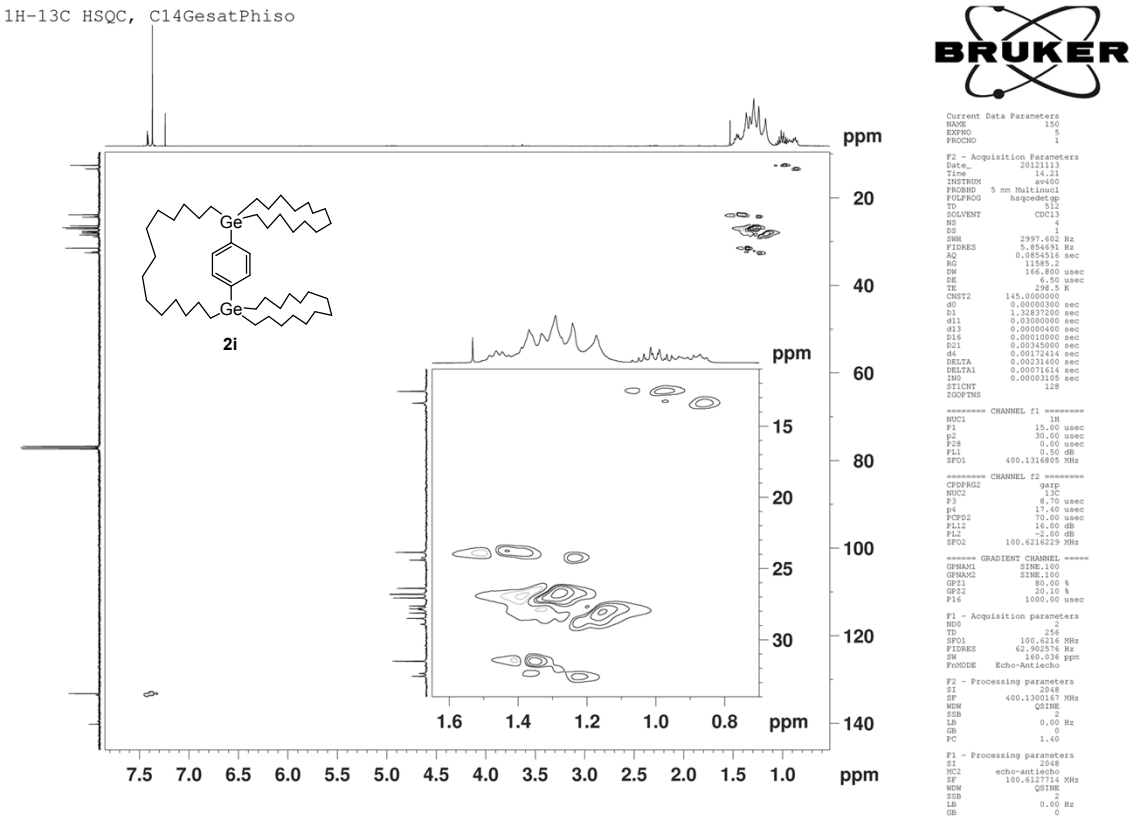

Fig S19. ^{1}H-^{13}C hsqc NMR spectrum of Molecular Gyrotop Isomer (**2i**) in $CDCl_3$.

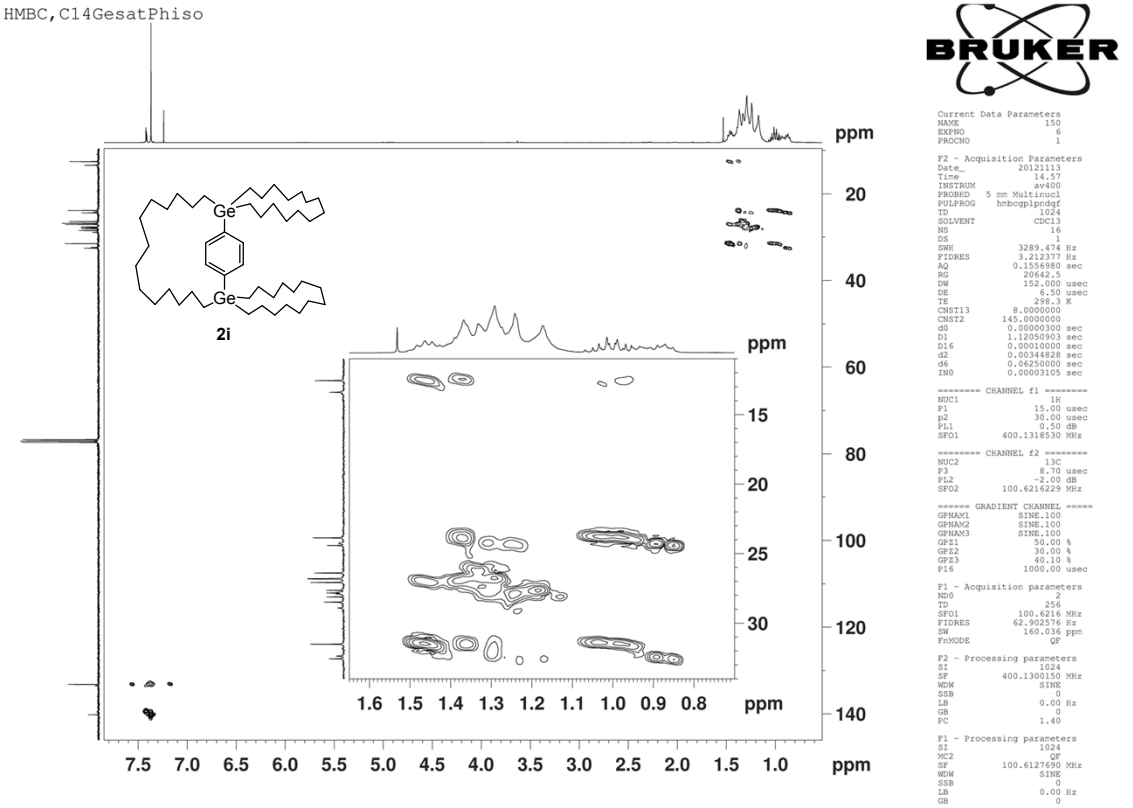

Fig S20. ^{1}H-^{13}C hmbc NMR spectrum of Molecular Gyrotop Isomer (**2i**) in $CDCl_3$.

2. ORTEP Drawing of Moleculr Gyrotop 2

The structures were refined using a SHELXL program package. Because of remarkably weak diffraction data at high temperature, it was difficult to refine the structure of the crystal adequately. Certain C-C distances and C-C-C angles of the alkyl chains were restrained by means of DFIX and DANG, respectively, because of the unresolved disorder.

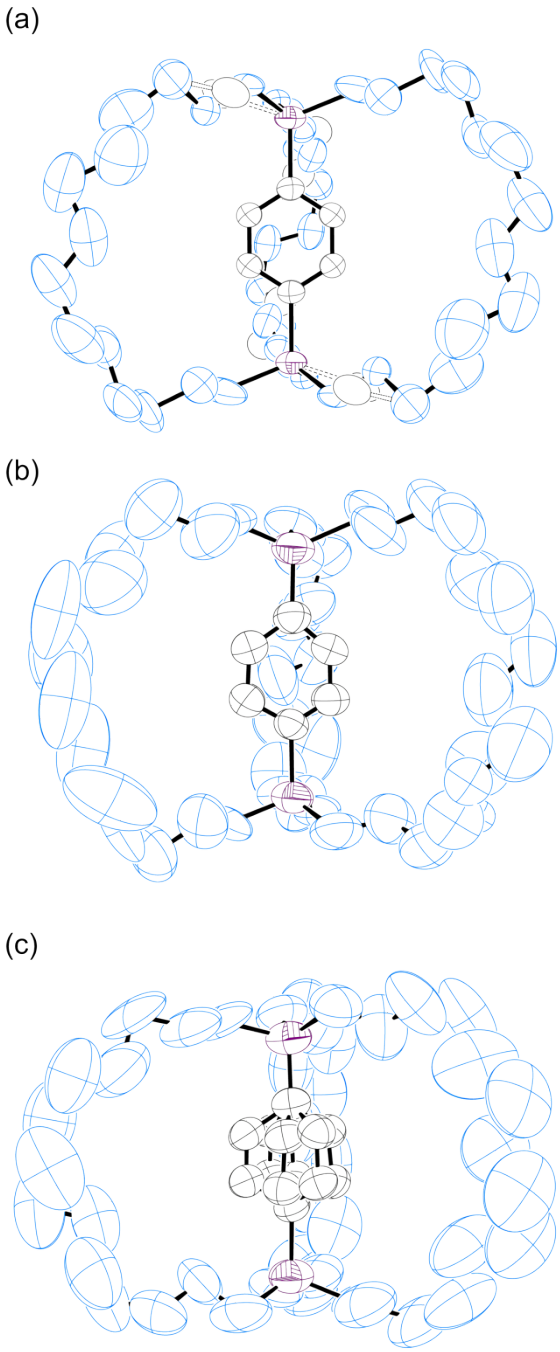

Fig S21. ORTEP drawing of the molecular structure of **2** at (a) 260 K; (b) 300 K; and (c) 340 K (30% thermal probability ellipsoid). Hydrogen atoms are omitted for clarity. Disorders of side chains are indicated.

Table S1. Crystal Data of **2** at 260 K, 300 K, and 340 K

		260 K	300 K	340 K
CCDC #		1026017	1026018	1026019
Empirical formula		C_{48} H_{88} Ge_2	C_{48} H_{88} Ge_2	C_{48} H_{88} Ge_2
Cryst shape		prism	plate	prism
Cryst color		colorless	colorless	colorless
Cryst size		0.40 x 0.20 x 0.20 mm^3	0.40 x 0.20 x 0.20 mm^3	0.40 x 0.20 x 0.20 mm^3
Formula weight / g mol^{-1}		810.36	810.36	810.36
Crystal system		Monoclinic	Monoclinic	Monoclinic
Space group		C2/c	Cc	Cc
Z		4	4	4
Temperature / K		260(2)	300(2)	340(2)
Cell parameter	*a*	25.736(7) Å	26.056(10) Å	26.170(17) Å
	b	11.733(3) Å	11.558(4) Å	11.561(8) Å
	c	18.790(5) Å	19.190(7) Å	19.398(13) Å
	α	90.00°	90.00°	90.00°
	β	120.046(3)°	118.979(4)°	118.837(7)°
	γ	90.00°	90.00°	90.00°
	V	4911(2) $Å^3$	5056(3) $Å^3$	5141(6) $Å^3$
Calculated density		1.096 Mg/m^3	1.065 Mg/m^3	1.047 Mg/m^3
F(000)		1760	1760	1760
Absorption coefficient		1.252 mm^{-1}	1.216 mm^{-1}	1.196 mm^{-1}
θ range for collecn (deg)		1.83 to 27.10°	2.43 to 16.30°	2.40 to 15.39°
Index ranges		-24<=h<=31, -8<=k<=14, -23<=l<=23	-24<=h<=30, -13<=k<=11, -22<=l<=22	-25<=h<=32, -14<=k<=11, -23<=l<=24
Reflections collected		11694	10770	11576
Independent reflections		4954 [R(int) = 0.0299]	6828 [R(int) = 0.0429]	7471 [R(int) = 0.0445]
Completeness		99.6 %	99.4 %	99.5 %
Goodness-of-fit on F^2		1.015	0.895	0.859
Final R indices [I>2sigma(I)]		R1 = 0.0640, wR2 = 0.1884	R1 = 0.0712, wR2 = 0.1778	R1 = 0.0585, wR2 = 0.1405
R indices (all data)		R1 = 0.1390, wR2 = 0.2352	R1 = 0.1889, wR2 = 0.2648	R1 = 0.2226, wR2 = 0.2312
Largest diff. peak and hole		0.439 and -0.311 e.$Å^{-3}$	0.358 and -0.176 e.$Å^{-3}$	0.177 and -0.094 e.$Å^{-3}$

3. Details of Solid-state ^{2}H NMR Study of 2-d_4

The temperature-dependent, solid-state ^{2}H NMR spectra of **2-d_4** were obtained through the same procedure as reported previously for **1-d_4**.[4e] The details are as follows: the data were recorded using a quadrupolar echo pulse sequence (d1-90° pulse-τ1-90° pulse-τ2-FID; 90° pulse = 4.2 μs, τ1 = 30 μs, τ2 = 20 μs, d1 = 20 s). Simulations of the ^{2}H NMR spectra were carried out using NMR-WEBLAB. The following parameters were used for the simulations: quadrupolar coupling constant $q$cc = 122 kHz, asymmetry parameter η = 0, line broadening = 3 kHz.

The temperature dependence of the spin-lattice relaxation time (T_1) in the ^{2}H NMR spectra was recorded using an inversion-recovery quadrupolar echo pulse sequence (d1-180° pulse-d2-90° pulse-τ1-90° pulse-τ2-FID; 90° pulse = 4.2 μs, τ1 = 30 μs, τ2 = 20 μs, d1 = 5–3 s, d2 varied) and standard T_1 analysis software. The spin-lattice relaxation time (T_1) was analyzed using the general relaxation model (eq. 1). T_1 is known to depend on the motional model for the exchange process; several special motions have been discussed so far.

a. VT-Solid state ^{2}H NMR spectra of 2-d_4.

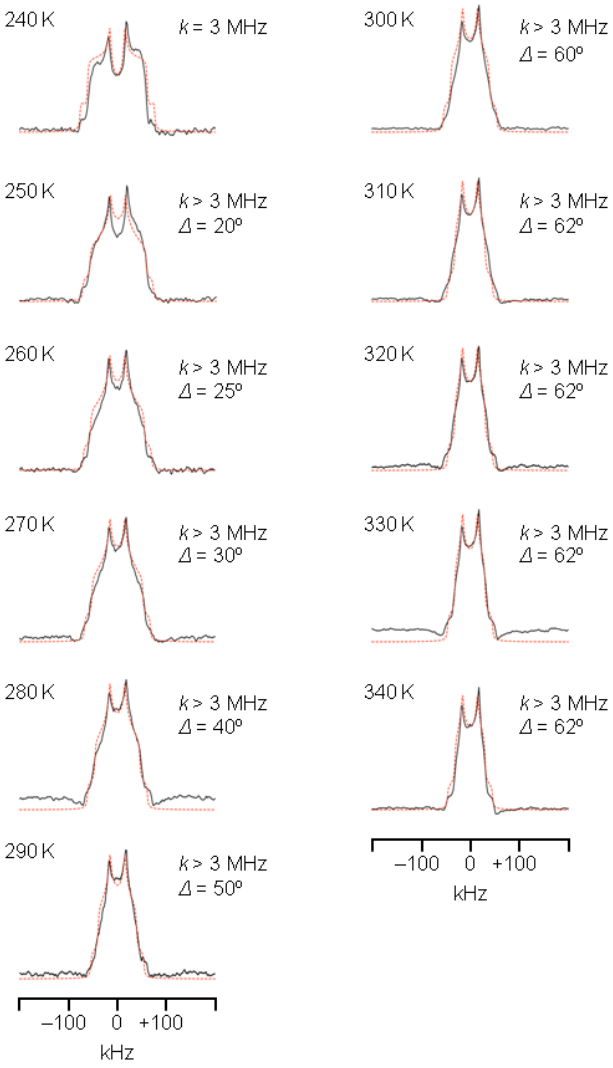

Fig S22. Temperature dependence of solid-state ^{2}H NMR spectra of **2-d_2** [solid black line: observed spectra; dotted red line: spectra simulated with designated exchange rate constants, k, and degree of angular displacement, Δ. The simulation model is mentioned in main text].

b. Analysis of temperature dependence of the ^{2}H NMR spin-lattice relaxation (T_1) measurements of **2**-d_2

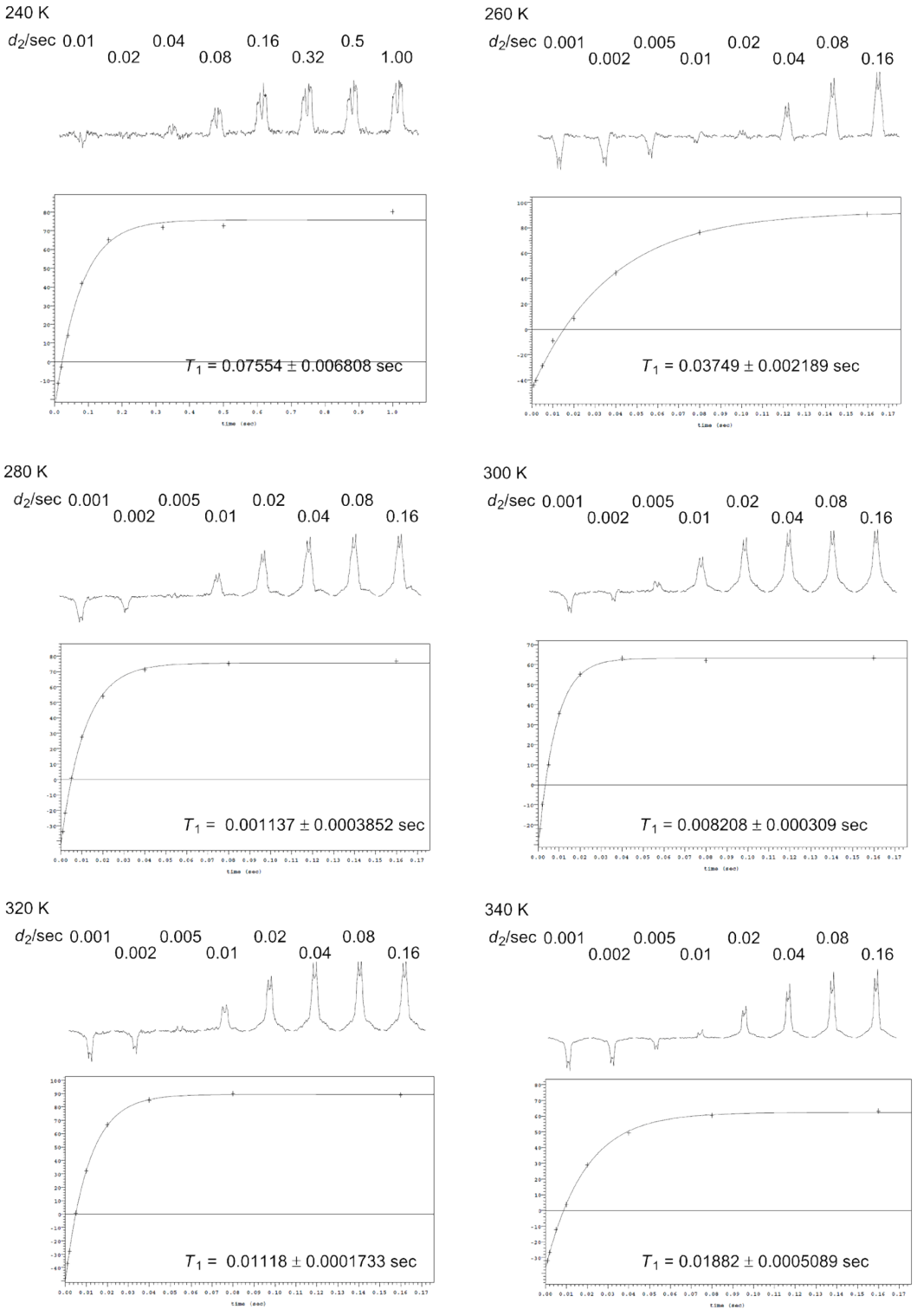

Fig S23. Representative inversion-recovery ^{2}H NMR spectroscopy data and single exponential fit from solid sample of molecular gyrotop **2**-d_4 (240 K – 340 K).

4. Details of Optical properties of a single crystal of 2

The fast and slow optical axes were confirmed by a polarized-light microscope equipped with a sensitive color plate. Retardations were observed by the polarized-light microscope equipped with a Berek compensator and monochromatic light at 546 nm generated by a color filter. The thickness of the crystal was measured by a laser displacement sensor at 300 K. The Δn value was calculated from the retardation/thickness of the sample.

a. Crystal orientation mapping of a single crystal of 2

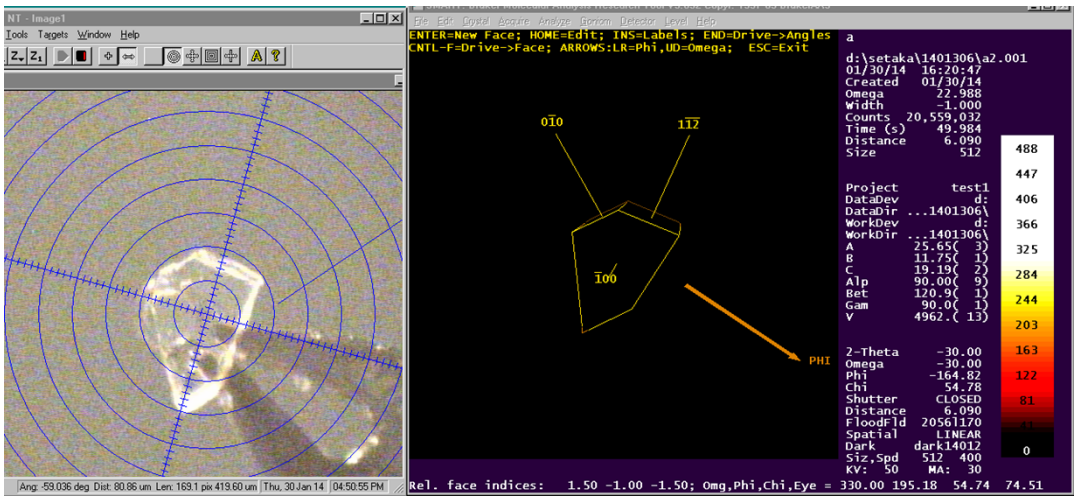

Fig S24. Crystal orientation mapping of a single crystal of **2** as determined by X-ray diffraction study at 300 K.

b. Thickness of the single crystal of 2

The thickness of the crystal was measured at 300 K using a laser displacement sensor (KEYENCE LT-9010M).

(a) (b) (c)

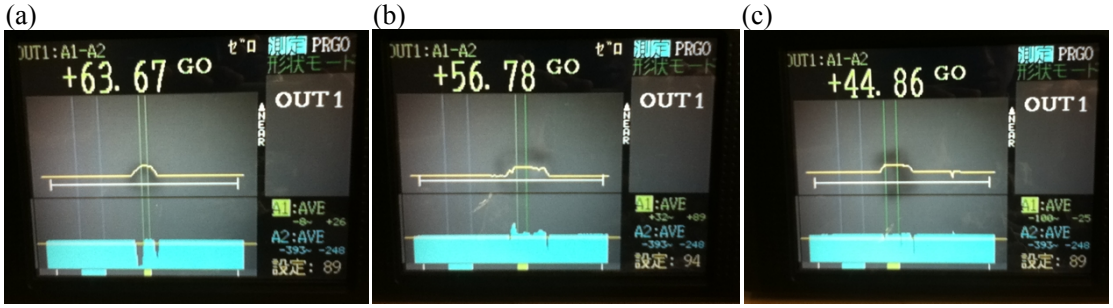

Fig S25. Measurement of the thickness of the single crystal of **2** at 300 K using a laser displacement sensor (KEYENCE LT-9010M); (a) 63.7 ± 1.0 μm;(b) 56.8 ± 1.0 μm; (c) 44.9 ± 1.0 μm.

c. Photograph of single crystals of 2 observed by polarized microscopy

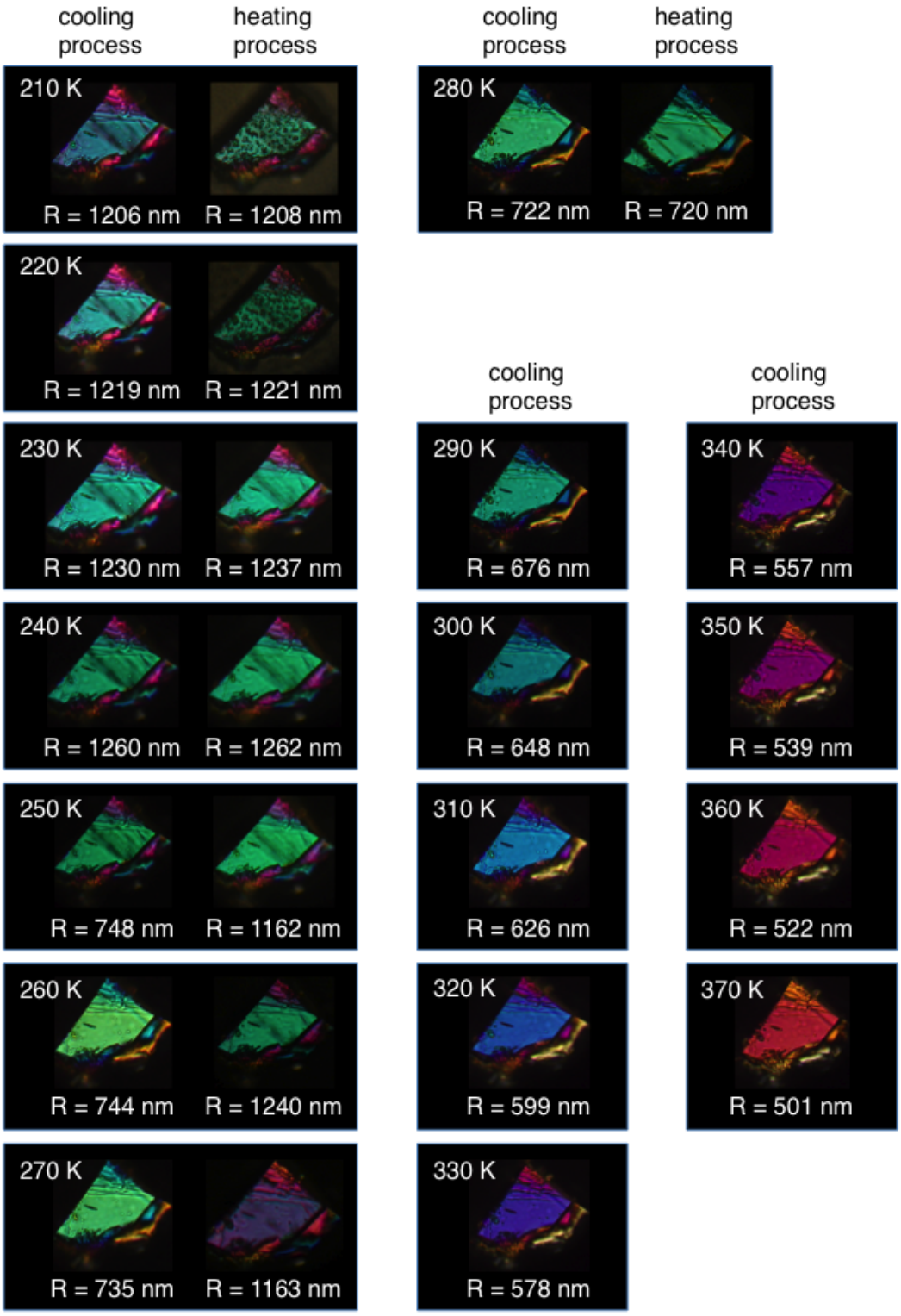

Fig S26a. Photographs of the single crystal of **2** (sample thickness: 64 ± 1 μm) showing the crystal face upon irradiation with polarized white light ({100} face at 200 K).

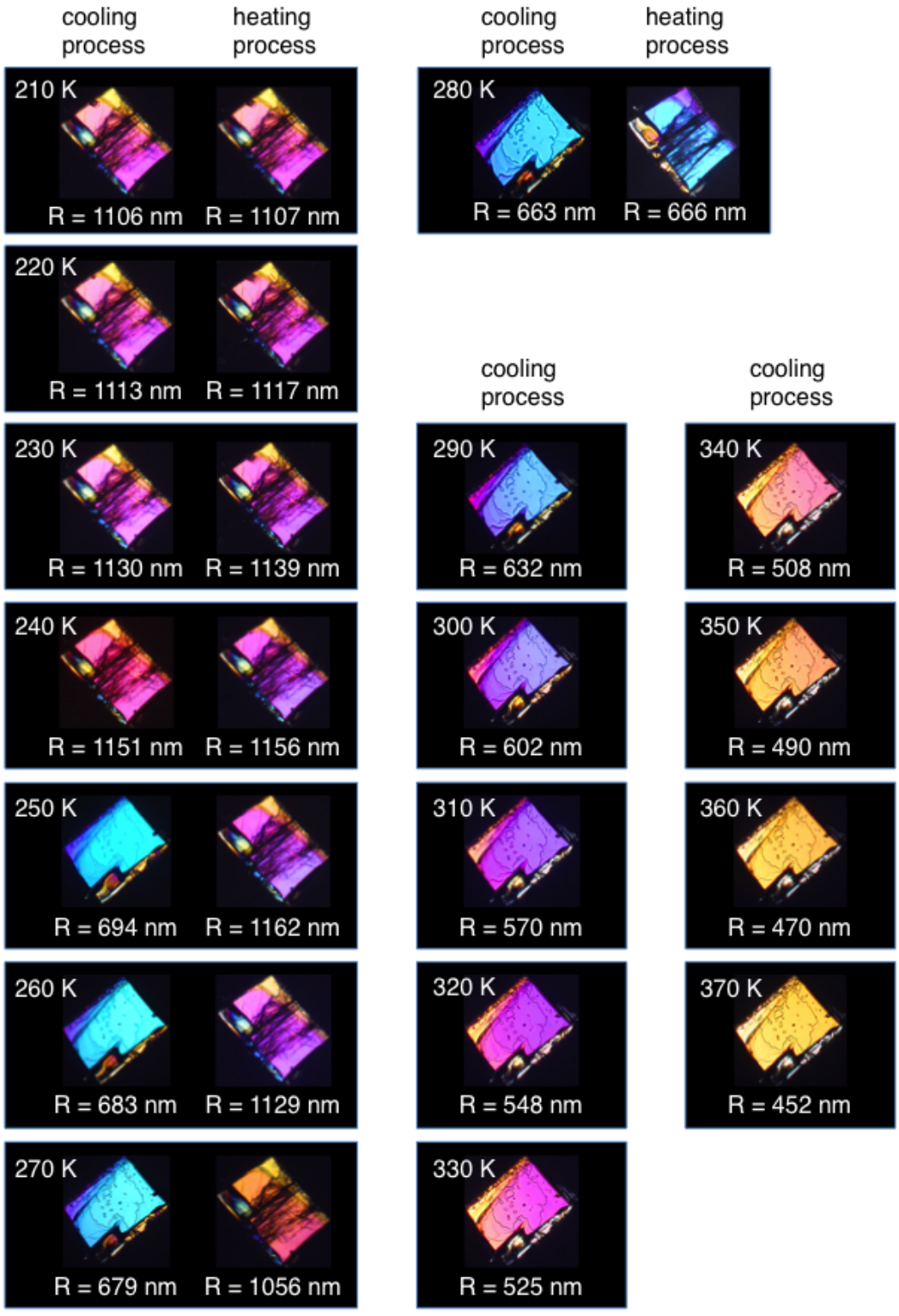

Fig S26b. Photographs of the single crystal of **2** (sample thickness: 57 ± 1 μm) showing the crystal face upon irradiation with polarized white light ({100} face at 200 K).

Fig S26c. Photographs of the single crystal of **2** (sample thickness: 45 ± 1 μm) showing the crystal face upon irradiation with polarized white light ({100} face at 200 K).

d. Temperature dependence of Δ*n* of 2

Temperature dependence of birefringence (Δ*n*) of the crystal face of a single crystal of **2**, calculated from Retardation/Thickness as summarized in Table S2.

Table S2-1. Temperature Dependence of Retardation, and Δ*n* of **2**.

(Thickness of the Single Crystal d = 44.9 μm)

Temperature / K	Retardation [1] / nm cooling process | heating process	Δ*n* [2] / 10^{-3} cooling process | heating process
210	855.7 | 859.7	19.08 ± 0.60 | 19.16 ± 0.53
220	871.5 | 864.1	19.43 ± 0.47 | 19.26 ± 0.57
230	880.3 | 876.4	19.63 ± 0.50 | 19.54 ± 0.47
240	897.8 | 885.4	20.02 ± 0.53 | 19.74 ± 0.54
250	546.2 | 892.5	12.18 ± 0.29 | 19.90 ± 0.55
260	544.5 | 872.3	12.14 ± 0.33 | 19.45 ± 0.49
270	536.4 | 540.7	11.96 ± 0.29 | 12.01 ± 0.33
280	526.5 | 528.0	11.74 ± 0.31 | 11.79 ± 0.28
290	497.2 | 499.2	11.08 ± 0.28 | 11.13 ± 0.28
300	473.6 | 472.5	10.56 ± 0.28 | 10.53 ± 0.28
310	451.9 | 451.4	10.07 ± 0.28 | 10.07 ± 0.25
320	432.1 | 435.5	9.63 ± 0.27 | 9.72 ± 0.23
330	417.7 | 418.1	9.31 ± 0.24 | 9.32 ± 0.23
340	405.1 | 400.5	9.03 ± 0.32 | 8.93 ± 0.28
350	385.3 | 387.6	8.59 ± 0.29 | 8.64 ± 0.26
360	371.6 | 369.9	8.28 ± 0.26 | 8.25 ± 0.23
370	357.2 | 357.3	7.96 ± 0.23 | 7.97 ± 0.24

1) Mean values of three time measurements.

2) The error for the birefringence Δ*n* includes both a measurement error of retardation and a thickness error (± 1.0).

(Thickness of the Single Crystal d = 56.8 μm)

Temperature / K	Retardation [1] / nm cooling process | heating process	Δn [2] / 10^{-3} cooling process | heating process
210	1105.6 | 1107.3	19.47 ± 0.43 | 19.50 ± 0.49
220	1112.5 | 1117.0	19.59 ± 0.47 | 19.67 ± 0.37
230	1129.6 | 1138.9	19.89 ± 0.49 | 20.06 ± 0.38
240	1151.3 | 1155.9	20.28 ± 0.42 | 20.36 ± 0.42
250	693.8 | 1162.0	12.22 ± 0.25 | 20.47 ± 0.45
260	683.4 | 1129.2	12.04 ± 0.24 | 19.89 ± 0.39
270	673.9 | 1056.0	11.87 ± 0.23 | 18.60 ± 0.48
280	663.1 | 666.0	11.68 ± 0.26 | 11.73 ± 0.32
290	631.7 | 628.3	11.13 ± 0.25 | 11.13 ± 0.25
300	601.1 | 599.4	10.60 ± 0.20 | 10.60 ± 0.20
310	570.2 | 571.0	10.04 ± 0.20 | 10.04 ± 0.20
320	548.1 | 548.6	9.65 ± 0.22 | 9.65 ± 0.22
330	524.7 | 526.5	9.24 ± 0.20 | 9.24 ± 0.20
340	508.4 | 506.5	8.95 ± 0.22 | 8.95 ± 0.22
350	489.5 | 489.1	8.62 ± 0.16 | 8.62 ± 0.16
360	470.2 | 470.2	8.28 ± 0.17 | 8.28 ± 0.17
370	452.1 | 449.5	7.96 ± 0.19 | 7.96 ± 0.19

1) Mean values of three time measurements.

2) The error for the birefringence Δn includes both a measurement error of retardation and a thickness error (± 1.0).

e. Details of measurement of the optical axes of the single crystal of 2

On the {100}-face of the crystal at 300 K, the fast optical axis is observed to be parallel to <010> axis as ascertained from the decrease in the retardation by 147 nm, observed using a polarized-light microscope equipped with a 1/4λ plate, which adds 147 nm along the <010> axis (FigS27(i)b). After rotation of the crystal by 90°, the retardation observed through the 1/4λ plate increased by 147 nm (Fig S27(i)c), indicating that the slow optical axis is perpendicular to <010> axis. On the other hand, in the case at 240 K the increment and decrement of the retardation observed through the 1/4λ plate were opposite to that observed at 300 K (Fig S27(ii)).

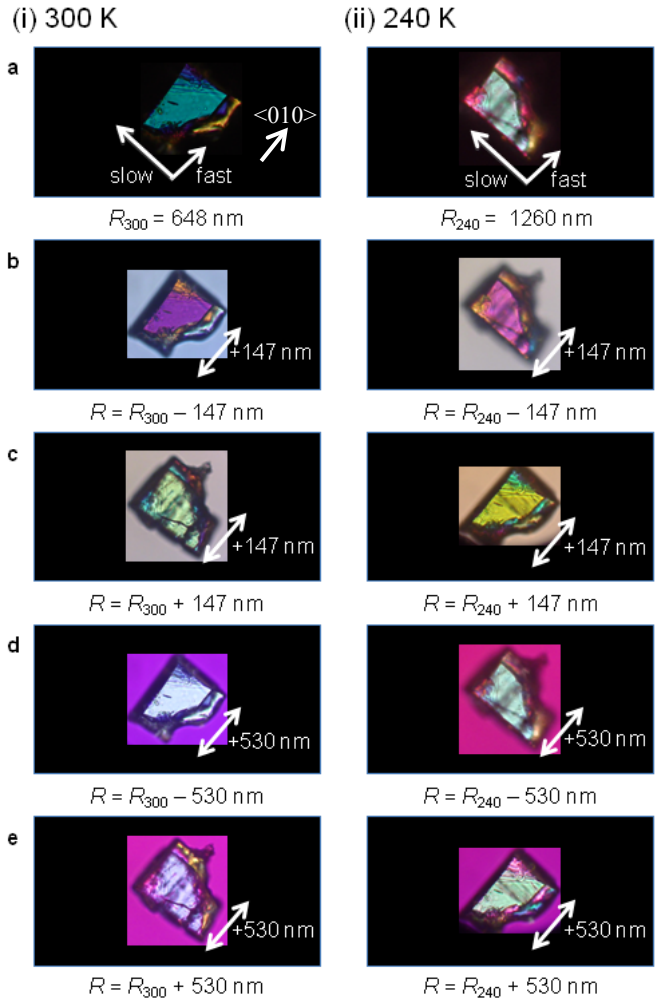

Fig S27. Photographs of the single crystals of **2** (sample thickness: 63.7 ± 1.0 μm) on the crystal face upon irradiation with polarized white light and its retardation (*R*) ({100} face at 300 K). **a**, Normal photograph with directions of optical axes. **b**, Photograph through a 1/4λ plate. **c**, Photograph through a 1/4λ plate after 90° rotation of the crystal. **d**, Photograph through a sensitive color plate. **e**, Photograph through a sensitive color plate after 90° rotation of the crystal.